



# Stable trimorphic coexistence in a lattice model of spatial competition with two site types

Ilmari Karonen\*

Department of Mathematics and Statistics, University of Helsinki, PO Box 68, FI-00014, Finland

## ARTICLE INFO

### Article history:

Received 29 December 2010

Received in revised form

13 October 2011

Accepted 17 October 2011

Available online 25 October 2011

### Keywords:

Coexistence mechanisms

Resource competition

Individual-based models

Lattice contact process

Spatial heterogeneity

## ABSTRACT

I examine the effect of exogenous spatial heterogeneity on the coexistence of competing species using a simple model of non-hierarchical competition for site occupancy on a lattice. The sites on the lattice are divided into two types representing two different habitats or spatial resources. The model features no temporal variability, hierarchical competition, type-dependent interactions or other features traditionally known to support more competing species than there are resources. Nonetheless, stable coexistence of two habitat specialists and a generalist is observed in this model for a range of parameter values. In the spatially implicit mean field approximation of the model, such coexistence is shown to be impossible, demonstrating that it indeed arises from the explicit spatial structure.

© 2011 Elsevier Ltd. All rights reserved.

## 1. Introduction

The coexistence of competing species, and factors promoting and limiting it, are of considerable practical and theoretical interest in ecology. A well known “rule of thumb” is the principle of competitive exclusion (Gause, 1932; Tilman, 1982; Levin, 1970), which states that at most  $n$  mutually competing species may stably coexist on  $n$  available resources.

Under suitable assumptions, the competitive exclusion principle can be proven as a mathematical theorem. However, if these assumptions are violated – for example, if the resource abundances may fluctuate over time, either due to external resources or simply because the ecological dynamics tend to a cyclic or chaotic attractor – it may no longer hold (although a related concept, the essential dimensionality of the environment (Dieckmann and Metz, 2006; Metz et al., 2008), may still be applied to such systems).

For systems which do satisfy these assumptions, the validity of the competitive exclusion principle depends fundamentally on just what we count as “a resource” (Abrams, 1988). This is not as simple a matter as it sounds. Were one to ask a practical-minded ecologist what constitutes a resource, they might name examples such as water, sunlight and nutrients for plants, or prey species for animals. But in the mathematically exact form of the competitive exclusion principle, almost anything may constitute a distinct resource: a single prey individual, a square meter of land,

a specific combination of nutrient concentrations, etc. Thus, even in systems which the competitive exclusion principle formally holds, the actual number of potentially coexisting competitors may be greater than one would expect by naively undercounting the resources.

The effect of spatial structure on the maximum diversity a system can support is, in particular, often neglected. For example, systems consisting of several distinct types of habitats are often modeled by assuming that each habitat constitutes a homogeneous patch within which the populations are well mixed. If competition between individuals is for suitable living space within these habitats, space in each habitat then becomes a single resource, and thus one would expect (and will, given these assumptions, mathematically discover) that at most  $n$  competitors may stably persist in  $n$  distinct habitats.

In reality, however, even if habitats are homogeneous, they are certainly not usually well mixed. Thus, individuals living near habitat boundaries will, over time, experience a different environment than those living in the interior of habitat patches. (Even if the individuals themselves do not move or interact with anything outside their local site, their offspring must still disperse and may end up in a different habitat.) This can create additional niches near habitat boundaries in which additional competing species might be able to coexist.

To demonstrate this, I present in this paper a simple spatially explicit toy model of site occupancy competition, which supports stable coexistence of three strains – two specialists and one generalist – on two spatially segregated habitats on a lattice of sites. This model contains no other features known to promote coexistence,

\* Tel.: +358 41 456 3263; fax: +358 9 1951 1400.

E-mail address: [ilmari.karonen@helsinki.fi](mailto:ilmari.karonen@helsinki.fi)

such as internally or externally generated temporal fluctuation (Hsu et al., 1978; Armstrong and McGehee, 1980), hierarchical site competition (Adler and Mosquera, 2000; Tilman, 1994), direct strain-dependent competition terms (Murrell and Law, 2003) or cooperative or other nonlinear interactions between individuals. Rather, the coexistence arises merely from the presence of habitat boundaries combined with passive distance-limited dispersal, which causes specialist strains to be locally maladapted near these boundaries and thereby allows more generalist strains to persist there.

As far as I know, this particular mechanism of coexistence has not been previously studied in individual-based models. A similar coexistence mechanism was very recently described in a reaction–diffusion model and in a one-dimensional stepping stone model by Débarre and Lenormand (2011), who termed it “habitat boundary polymorphism”. The results in this paper parallel theirs, and confirm that this mechanism is robust with respect to the details of the model, provided that the basic features of habitat heterogeneity and passive distance-limited dispersal are present.

A model almost identical to mine was studied by Lanchier and Neuhauser (2006), who showed analytically that it could support stable dimorphic coexistence, either of a generalist and a specialist strain or of two different specialist strains. My model differs from theirs only in that they restrict the habitat configuration to the special case of an infinite regular checkerboard pattern consisting of  $n$ -by- $n$  squares of each habitat type.<sup>1</sup> However, while Lanchier and Neuhauser did briefly remark that “the generalists persist for a very long time along the boundaries ... where the density of specialists is low” in numerical simulations, they do not seem to have investigated this possibility of trimorphic coexistence in their model further. Similarly, Snyder and Chesson (2003) define a model quite similar to mine (although in discrete time and one spatial dimension), and observe the enhancing effect of stable spatial heterogeneity and local dispersal on coexistence of competitors, but also restrict their analysis to two competitors.

## 2. Model definition

I model a population of haploid, asexually reproducing sessile organisms with distance-limited offspring dispersal. The model I’ll define below belongs to the class of lattice contact processes (Harris, 1974; Neuhauser, 1992), in which the environment is taken to consist of a lattice of discrete sites, and interactions are (mainly) between nearest neighbor sites.

Let  $L$  be a regular two-dimensional lattice of sites (e.g.  $L = \mathbb{Z}^2$ , although for numerical simulations a finite lattice must obviously be used). To each site I assign a random, fixed habitat class (“A” or “B”), such that both classes of sites are present in  $L$  in equal numbers. (I will describe the way in which the habitat classes are assigned in more detail below.)

Each site in  $L$  may, at a given time, be either vacant or occupied by an individual belonging to one of three strains: an A-specialist ( $a$ ), a B-specialist ( $b$ ) or a generalist ( $g$ ). The two specialist strains can only occupy sites in their respective habitat class, while the generalist strain may occupy any site.

Except for their different habitat adaptations, the strains are completely identical: all individuals die with rate  $\mu$  and produce offspring with rate  $\phi$ . Offspring are randomly dispersed to the eight nearest sites surrounding the parent individual’s site (or possibly, with probability  $\epsilon$ , to a randomly chosen site in  $L$ ), and will become new individuals if the site they land in is vacant and of a suitable habitat class. However, the generalists pay a cost

for their ability to live in either habitat: their offspring survive only with probability  $p_g < 1$ .<sup>2</sup>

The time evolution of the entire lattice  $L$  can thus be considered as a continuous-time Markov process, whose state at time  $t$  is a function  $\eta_t : L \rightarrow \{0, a, b, g\}$  mapping sites in  $L$  to their occupancy state (with the state 0 denoting a vacant site). The local transition rates of a site  $x$  are then

$$\begin{aligned} r(0 \rightarrow a) &= \mathbf{1}_{\{H_x = A\}} \phi \left( (1-\epsilon) \sum_{y \in E_x} \frac{\mathbf{1}_{\{\eta_t(y) = a\}}}{|E_y|} + \epsilon \sum_{y \in L} \frac{\mathbf{1}_{\{\eta_t(y) = a\}}}{|L|} \right), \\ r(0 \rightarrow b) &= \mathbf{1}_{\{H_x = B\}} \phi \left( (1-\epsilon) \sum_{y \in E_x} \frac{\mathbf{1}_{\{\eta_t(y) = b\}}}{|E_y|} + \epsilon \sum_{y \in L} \frac{\mathbf{1}_{\{\eta_t(y) = b\}}}{|L|} \right), \\ r(0 \rightarrow g) &= p_g \phi \left( (1-\epsilon) \sum_{y \in E_x} \frac{\mathbf{1}_{\{\eta_t(y) = g\}}}{|E_y|} + \epsilon \sum_{y \in L} \frac{\mathbf{1}_{\{\eta_t(y) = g\}}}{|L|} \right) \end{aligned} \quad (1)$$

and

$$r(a \rightarrow 0) = r(b \rightarrow 0) = r(g \rightarrow 0) = \mu,$$

where  $r(s \rightarrow s')$  is the rate at which a site in state  $s$  changes to state  $s'$ ,  $H_x$  is the habitat class of site  $x$  and  $E_x$  is the set of sites adjacent to  $x$ .

The behavior of the model is determined by the habitat configuration along with two parameters: the scaled baseline fecundity rate  $\lambda = \phi/\mu$  (or equivalently, the scaled mortality rate  $\lambda^{-1} = \mu/\phi$ ) and the generalist survival rate  $p_g$ . The baseline fecundity affects the equilibrium population density of both the specialists and the generalist strain: at low  $\lambda$  all strains die out, while at very high  $\lambda$  almost all sites are occupied at any time.

The parameter  $0 < p_g < 1$  determines the penalty which the generalist must pay for its ability to exploit both site types, and is (together with the habitat configuration) crucial in determining the outcome of the model. If  $p_g$  is too low, the generalist strain will not be viable, or, even if viable on its own, may lose in competition to the specialists. Conversely, if  $p_g$  is close to 1, the specialist strains gain little or no advantage over the generalist from their specialization, while paying a considerable price in being able to live in only one habitat, and can thus be expected to lose to the generalist.

## 3. Landscape generation

An issue so far overlooked in the model definition above is the way in which the lattice sites are assigned to their habitat classes. The simplest way to do so, of course, is to simply assign each site independently to either habitat with equal probability. This produces a lattice with no correlations between the habitat classes of different sites.

However, real environmental features are often correlated, and it would be desirable to consider the effects of such correlations on the behavior of the model. To first order, such correlations can be characterized by the pairwise correlation probability  $k = \Pr[H_x = H_y | y \in E_x]$ , i.e. the probability that two randomly chosen adjacent sites have the same habitat type. With an equal number of sites in each habitat, the pairwise correlation probability on a completely random, uncorrelated lattice is  $k = \frac{1}{2}$ , while lattices with  $\frac{1}{2} < k < 1$  are positively correlated and those with  $0 < k < \frac{1}{2}$  are anticorrelated.<sup>3</sup>

To generate random habitat class distributions with a given pairwise correlation probability for numerical simulations, I start by

<sup>2</sup> Equivalently, I could have scaled the offspring production rate of the generalists to  $p_g \phi$ . However, the definition I have chosen allows a straightforward generalization to semi-specialist strains with different (non-zero) survival rates in different habitats.

<sup>3</sup> On a square lattice where each site is adjacent to its eight nearest neighbors, the smallest achievable value of  $k$  is  $\frac{1}{4}$ .

<sup>1</sup> Lanchier and Neuhauser (2006) also consider a somewhat different set of dispersal kernels, but both theirs and mine include the basic case of strict nearest-neighbor dispersal.

randomly choosing half of the sites and assigning them to habitat A and the rest to habitat B. I then apply an iterative annealing process, which reassigns randomly chosen sites to new habitat classes with suitable weighted probabilities, until the desired value of  $k$  is reached.

There are many possible variations of the general annealing scheme I have used. The basic idea in all of them is to change the habitat classes of randomly chosen sites if this would change  $k$  in the desired direction, while occasionally also allowing changes in the other direction so that the process does not get stuck at a local minimum or maximum.

The particular annealing algorithm I have used to generate habitat configurations for the simulations in this paper<sup>4</sup> chooses random adjacent pairs of sites, and swaps their habitat classes with probability

$$p = \frac{d^\gamma}{d^\gamma + (1-d)^\gamma}$$

if  $k_{\text{current}} < k_{\text{target}}$ , or with probability  $1-p$  otherwise, where  $d$  is the fraction of sites adjacent to the chosen pair which belong to the opposite habitat than their neighbor in the chosen pair.

The exponent  $\gamma$  is a free parameter which controls the “temperature” of the process. When  $\gamma = 1$ , the probability of exchanging the habitat classes of a chosen site pair is a linear function of  $d$ . This tends to produce fairly slow convergence and rough, jagged cluster boundaries. At high values of  $\gamma$ ,  $p$  approaches a step function, producing faster initial convergence and smoother cluster boundaries, but also increasing the risk of the process getting stuck at a local maximum or minimum of  $k$ .

#### 4. Mean field approximation

Classical ecological theory predicts that the only possible outcome of three distinct strains competing for the occupancy of two habitats should be the eventual extinction of one or more of the strains, except at specific degenerate choices of the model parameters where neutral coexistence may occur. I will demonstrate below that this prediction indeed holds if the populations are assumed to be well mixed, either globally or within each habitat. However, I shall also show that, in the full model with explicit spatial structure, a region of stable trimorphic coexistence does exist for intermediate values of  $p_g$ .

Assuming that all offspring disperse uniformly over the entire lattice, i.e. that  $\epsilon = 1$  in (1), the transition rates of each site are fully described by the mean population densities  $n_a$ ,  $n_b$  and  $n_g$  of the different strains, where

$$n_s = \sum_{y \in L} \frac{\mathbf{1}_{\{n(y)=s\}}}{|L|}$$

for each strain  $s$ . Further letting the lattice size  $|L|$  tend to infinity, one obtains a simple system of ordinary differential equations describing the time evolution of these mean population densities – the so called *mean field* approximation – which may be solved analytically. Such an approximation of an essentially equivalent model was presented by Lanchier and Neuhauser (2006), who showed that trimorphic coexistence was only possible for degenerate choices of parameter values.

However, simply assuming all dispersal to be global completely neglects not only the detailed spatial habitat structure, but even the pairwise correlation parameter  $k$ . A better approximation, similar to the “improved mean field approximation” of Hiebeler and Morin (2007), is obtained by assuming well mixing

only within each habitat. The resulting approximation can be interpreted as a model of a population inhabiting two well-mixed habitat patches with a fraction  $k$  of all offspring remaining within their parent’s patch and the rest dispersing to the other patch. This *two-patch approximation* takes into account the habitat correlation parameter  $k$  but still retains the analytical tractability of the mean field approximation. (For  $k = \frac{1}{2}$ , the two approximations are exactly equivalent.) Below, I will analyze this approximation of the model defined above, and show that it also only supports non-degenerate coexistence of at most two strains.

Assume that the occupancy states of the lattice sites are independent, and that the probability of a site being occupied by a given strain  $s$  is equal to the mean population density  $n_{s,H}$  of that type in the site’s habitat  $H$ . Then, in the limit as  $|L| \rightarrow \infty$ , the time evolution of the population densities can be written as

$$\frac{d}{dt} n_{s,A} = p_{s,A} v_A \phi(k n_{s,A} + (1-k) n_{s,B}) - \mu n_{s,A},$$

$$\frac{d}{dt} n_{s,B} = p_{s,B} v_B \phi(k n_{s,B} + (1-k) n_{s,A}) - \mu n_{s,B}$$

for  $s \in \{a, b, g\}$ , where  $v_A$  and  $v_B$  are the vacant site densities in the two habitats and  $p_{s,A}$  and  $p_{s,B}$  are the probabilities of an offspring of type  $s$  surviving in the respective habitats:

$$p_{a,A} = p_{b,B} = 1,$$

$$p_{b,A} = p_{a,B} = 0,$$

$$p_{g,A} = p_{g,B} = p_g.$$

Equivalently, this system may be written in matrix form as

$$\frac{d}{dt} \bar{n}_s = M_s \bar{n}_s$$

for  $s \in \{a, b, g\}$ , where  $\bar{n}_s = [n_{s,A}, n_{s,B}]^T$  and

$$M_s = \begin{bmatrix} \phi k p_{s,A} v_A - \mu & \phi(1-k) p_{s,A} v_A \\ \phi(1-k) p_{s,B} v_B & \phi k p_{s,B} v_B - \mu \end{bmatrix}.$$

If this system has a nontrivial interior equilibrium  $\bar{n}_s$ , this necessarily implies that  $M_s \bar{n}_s = [0, 0]^T \neq \bar{n}_s$ , and therefore that  $M_s$  must be singular, and thus have a zero determinant, for each strain  $s$  present in the population. Writing out the determinant as

$$|M_s| = \phi^2 (2k-1) p_{s,A} v_A p_{s,B} v_B - \phi \mu k (p_{s,A} v_A + p_{s,B} v_B) + \mu^2 = 0$$

yields, for each  $s$ , an equation containing the same two unknown variables:  $v_A$  and  $v_B$ . As the coefficients  $p_{s,A}$  and  $p_{s,B}$  will, in general, be different for each strain  $s$ , one can see that, except for degenerate choices of the parameter values, no solution will exist for more than two strains.

More specifically, we can see that, in the absence of specialists, small generalist populations can grow in the two-patch approximation of this specific model if and only if  $p_g \phi > \mu$ , and conversely that small populations of either specialist strain can grow in the absence of the generalist if and only if  $k \phi > \mu$ . Outside these regions, shown in Fig. 1, the respective strains are not viable and will always die out (as the per capita growth rates in this model are always maximized at vanishing population densities).

Within the region where all strains are viable, the approximated model has (in general) two possibly stable equilibria: one where only the generalist is present, and one where the generalist is absent and both specialists present. (Any equilibria with only one specialist present are obviously unstable against invasion by the other specialist.) The former is stable if and only if  $p_g > k$ , while the latter is stable if and only if  $p_g < k$ . Only at exactly  $p_g = k$ , shown as the white line in Fig. 1, both of the equilibria are neutrally stable, and are connected by a line of neutrally stable equilibria along which neutral coexistence can occur.

<sup>4</sup> The interactive Java applets from which the snapshots in Fig. 6 are taken use a different annealing algorithm.

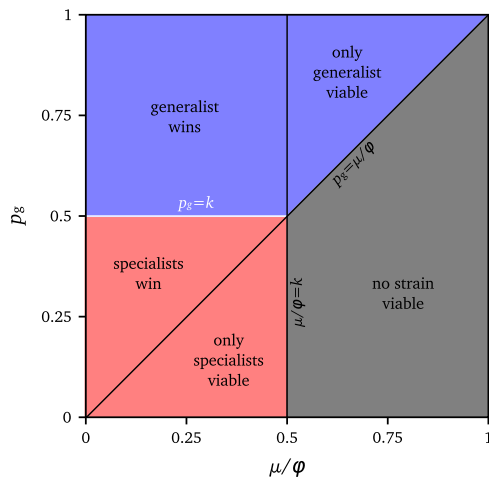


**Fig. 1.** The outcome of the model as predicted by the two-patch approximation for different values of the normalized mortality rate  $\mu/\phi$  and the generalist survival probability  $p_g$ . The diagonal line at  $\mu/\phi = p_g$  and the vertical line at  $\mu/\phi = k$  mark the boundaries at which the generalist and specialist strains go extinct even in the absence of competitors. In the regions marked “generalist wins” and “specialists win”, all strains can survive in the absence of competitors, but from any initial state with all three strains present, the system converges to either a monomorphic generalist-only state or a dimorphic specialist-only state. Along the white line at  $p_g = k$ , the three strains can coexist neutrally.

## 5. Simulation results

Studying the dynamics of the full unapproximated model requires numerical simulations. As such simulations tend to be computationally intensive, I have carried them out using custom, optimized programs written in the C programming language.<sup>5</sup> The simulation code used for this paper includes two variants of the coupling-based simulation algorithm described in Karonen (in preparation), one using an occupancy list for low population densities, and another using a vacancy list for high densities, with the outer simulation loop periodically checking the population density and switching to the variant with the higher mean time step per iteration. I have also ported the basic simulation code (without the coupling technique) to Java for demonstration purposes using interactive applets.

All simulation runs for this paper were done on a square  $256 \times 256$  lattice with eight neighbors per site and with the edges wrapping around to the opposite sides. In all simulation runs, time has been scaled so that the *per capita* mortality rate  $\mu = 1$ ; in effect, I measure time in mean individual lifetimes. Habitat configurations were generated using an annealing method as described in Section 3. The “flea” pseudorandom number generator (Jenkins, 2007) was used to produce random numbers, although I also carried out tests using other random number generators to check that the results did not depend on such details.

Fig. 2 shows the equilibrium densities of generalists and specialists observed in repeated individual-based simulations of the model on a  $256 \times 256$  lattice with reproduction to eight nearest neighbors and wrapped edges with an uncorrelated habitat distribution and a moderate value of  $\phi/\mu$ . Each simulation run was started from a random habitat configuration and a random initial state with half the sites occupied by generalists and half by specialists. Populations were allowed to equilibrate for  $50\,000/\mu$  time units, after which population densities were averaged over another  $50\,000/\mu$  time units. The specialist occupancy fractions are summed over both specialist strains.

Contrary to the predictions from the mean field approximation, a non-degenerate region of the parameter space where all

three strains stably coexist can be seen in Fig. 2. This region is displayed more extensively in Figs. 3 and 4, which plot the observed region of coexistence against  $\mu/\phi$  and  $p_g$  for the various habitat configurations (anticorrelated, uncorrelated and two positively correlated patterns) shown in Fig. 5. Fig. 3 shows results for pure nearest-neighbor dispersal ( $\epsilon = 0$ ), while in Fig. 4, 1% of all offspring were permitted to disperse uniformly over the whole lattice ( $\epsilon = 0.01$ ).

For Figs. 3 and 4, each simulation run was started from a random initial population on the fixed pregenerated habitat landscapes shown in Fig. 5. Populations were allowed to equilibrate for  $20\,000/\mu$  time units, after which population densities were averaged over  $2000/\mu$  time units. The red areas labelled “specialists win” and “only specialists viable” show where only the specialist strains survived, while in the blue regions labelled “generalist wins” and “only generalist viable” only the generalist strain remained. The lighter shaded area between them shows the part of the parameter space where both specialists and generalists survived with the color gradient shown above the figures indicating the relative average population densities.

In both Figs. 3 and 4, the region of stable coexistence can be seen as a more or less wedge-shaped area starting from the point where the viability boundaries of the strains intersect, which is where the two-patch approximation would predict a line of neutral coexistence (see Fig. 1). The main difference between the figures can be seen in the lower left side of the coexistence region: with global dispersal, the lower boundary of the coexistence region is quite sharp, whereas with no global dispersal and high baseline fecundity  $\phi/\mu$ , the generalist can often survive in small numbers (shown as a light orange hue in the plots) even where the specialist dominates.

This happens simply because the high fecundity allows even small isolated population clusters to survive for a long time, and because the strictly local dispersal prevents the specialists from recolonizing isolated habitat patches. If such a habitat patch happens to end up with no specialist individuals (either because all happen to die out, or because none were present initially), the patch can be colonized by generalists, which are then safe from competition there. Allowing a fraction of offspring to disperse globally lets the specialist strains recolonize such patches, eliminating this effect.

It can also be seen that the addition of global dispersal generally reduces the width of the coexistence region somewhat, although (except for the isolated patch effect noted above) the reduction is not yet very large for  $\epsilon = 0.01$ . This is to be expected, given that at  $\epsilon = 1$  the coexistence region reduces to a line, as shown by the mean field (and two-patch) approximation above.

The results shown in Figs. 2–4 were calculated using a simulation technique based on monotone coupling (Karonen, in preparation), which allows the system to be efficiently simulated for all values of the parameter  $p_g$  in parallel. Each line in Fig. 2 and each vertical stripe (out of 1024 per plot) in Figs. 3 and 4 corresponds to one simulation run. Because the simulation technique used causes the effects of random demographic fluctuations on populations with different values of  $p_g$  within the same run to be correlated, the results show stronger correlations within each run than between runs, which should be kept in mind when interpreting the figures.

Fig. 6 contains snapshots of simulations run on lattices with different site type patterns. It can be seen that, when sites of the same type are strongly clustered, large contiguous clusters are dominated by the respective specialist strain, while the generalist strain is able to persist in areas near cluster boundaries and in isolated minor clusters too small to support a stable specialist population.

On the other hand, when site types are uncorrelated, a different pattern is observed. Such lattices contain no large contiguous clusters that could be dominated by one specialist strain; instead,

<sup>5</sup> Source code available from author under an open source license.

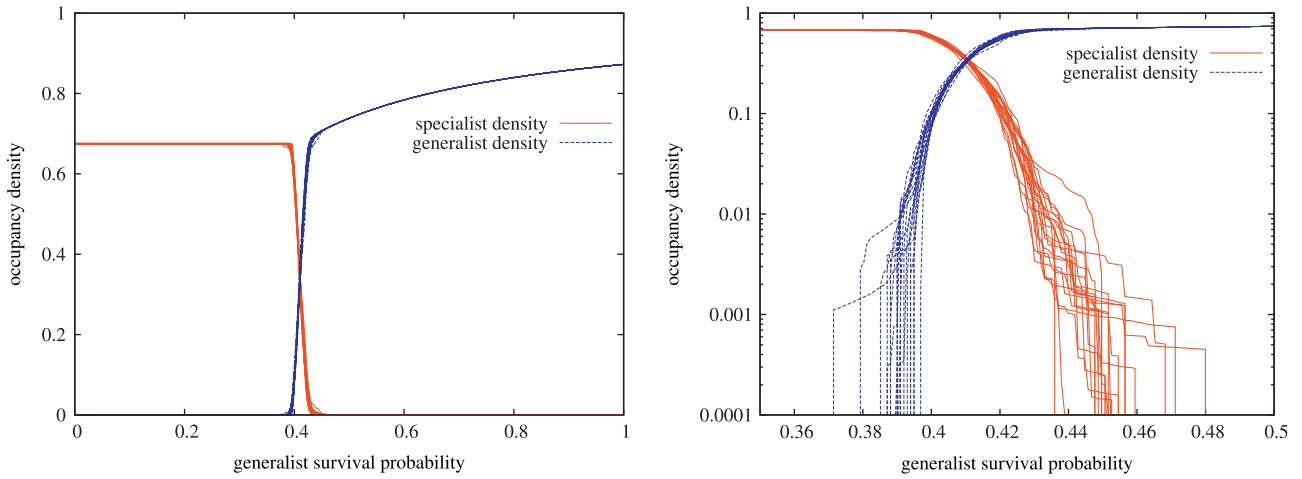


**Fig. 2.** Plots of equilibrium specialist and generalist densities at  $k=0.5$  and  $\phi = 8\mu$  as functions of  $p_g$  obtained from 20 numerical simulation runs. See text for details. The graph on the right has been plotted on a logarithmic scale and zoomed in to better show the coexistence region.

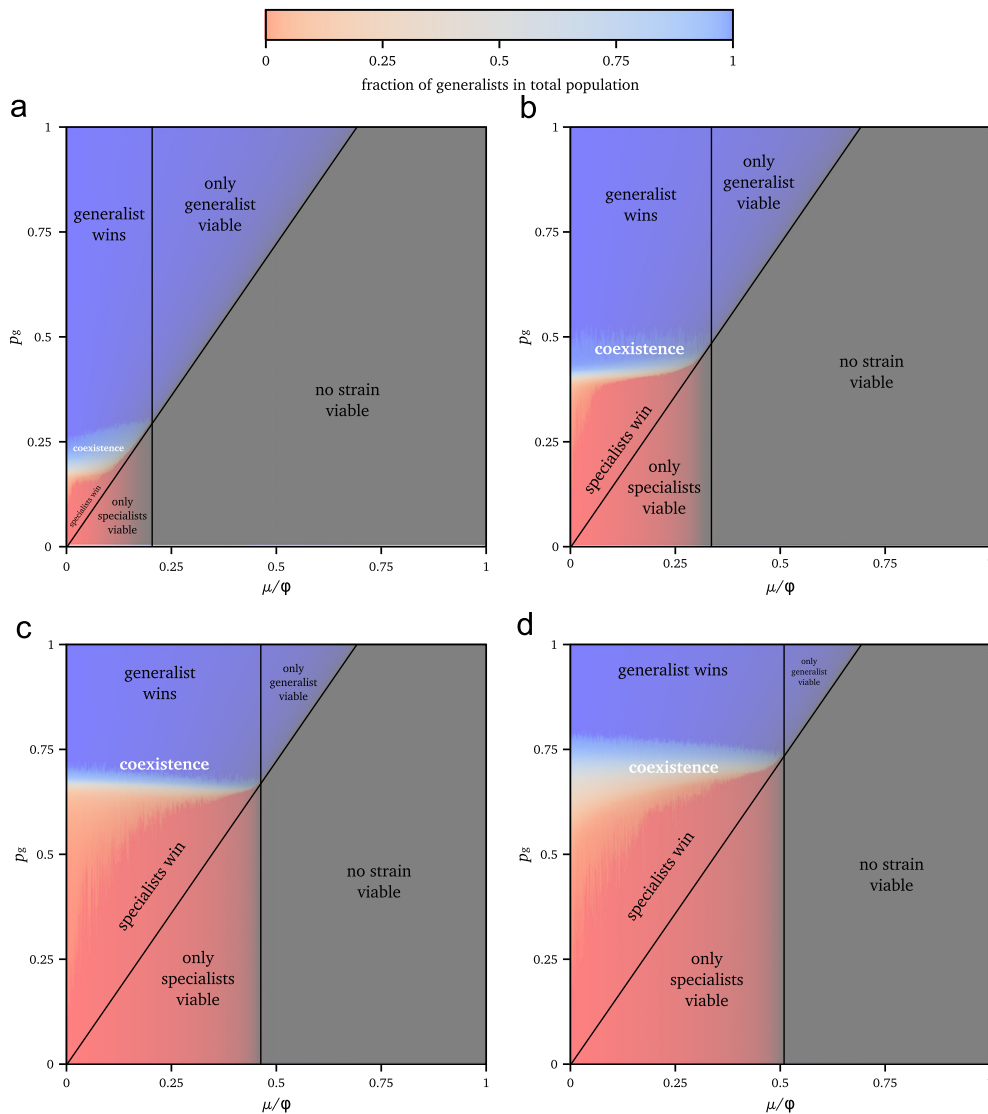


**Fig. 3.** Results of numerical simulations on a  $256 \times 256$  site lattice as functions of  $\mu/\phi$  and  $p_g$  on the habitat patterns from Fig. 5 with no global dispersal ( $\epsilon = 0$ ). See text for details. Compare with Fig. 4 and with the mean field predictions from Fig. 1. (a)  $k=0.3$ . (b)  $k=0.5$ . (c)  $k=0.75$ ,  $\gamma = 10$ . (d)  $k=0.75$ ,  $\gamma = 3$ .

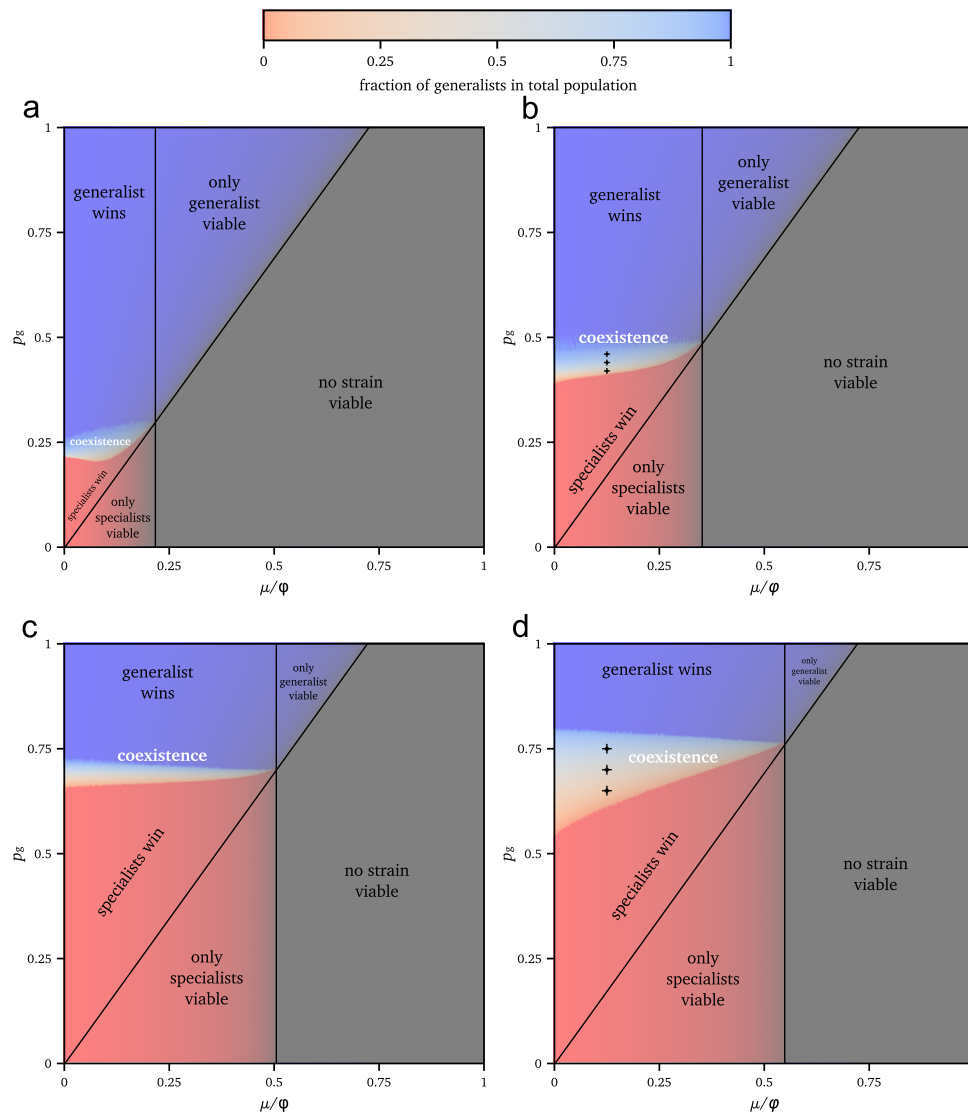


**Fig. 4.** Results of numerical simulations on a  $256 \times 256$  site lattice as functions of  $\mu/\phi$  and  $p_g$  on the habitat patterns from Fig. 5 with occasional global dispersal ( $\epsilon = 0.01$ ). See text for details. The marks on Fig. 4b and d show the parameter values used for the invasion simulations in Fig. 7. Compare with Fig. 3 and with the mean field predictions from Fig. 1. (a)  $k=0.3$ . (b)  $k=0.5$ . (c)  $k=0.75$ ,  $\gamma = 10$ . (d)  $k=0.75$ ,  $\gamma = 3$ .

the two specialist strains tend to occur together in regions where the random distribution of site types happens to favor one or both of them. Through competition with the generalist strain, the two specialist strains indirectly support one another, even though there is no direct interaction between them.

## 6. Mutual invasibility

To a skeptical mind, the results presented above may yet leave some doubt about whether the apparent coexistence observed in these simulations is indeed genuinely stable, or merely an artifact of slow convergence and insufficient simulation time. After all, if the simulation was run for long enough on a finite lattice, *eventually* one of the strains (and eventually all of them) would almost surely go extinct simply due to demographic stochasticity. Thus, it may not even be entirely clear what “stable coexistence on a finite lattice” should actually mean.

On an infinite lattice, as in Lanchier and Neuhauser (2006), a set of strains may be said to coexist stably if they can all persist indefinitely long with non-zero probability. By this definition, no

stable coexistence (or even just existence) is possible in a finite system. However, since there do exist known results that relate the scaling of the expected time to extinction on a finite lattice, as a function of lattice size, to the limiting behavior of the model on an infinite lattice, one might be inclined to try and use such scaling laws to extrapolate stability from small lattices to the infinite limit.

This is not the approach I have taken. After all, real habitats and populations, like the simulations employed in this paper, are finite—in appealing to a definition of coexistence that only works for infinite populations, one ends up obscuring the fact that, in reality, if a population of tens of thousands of individuals persisting over equally many generations is not considered stable, it’s hard to say what should be.

Rather, I wish to demonstrate the stability of the trimorphic coexistence in my model in a more direct manner, by showing that it exhibits *mutual invasibility*. That is to say, if a small number of individuals of any of the three strains are introduced into a stable population consisting solely of the other two strains, the introduced strain will, with positive probability, survive and grow in number up to its equilibrium density in the trimorphic

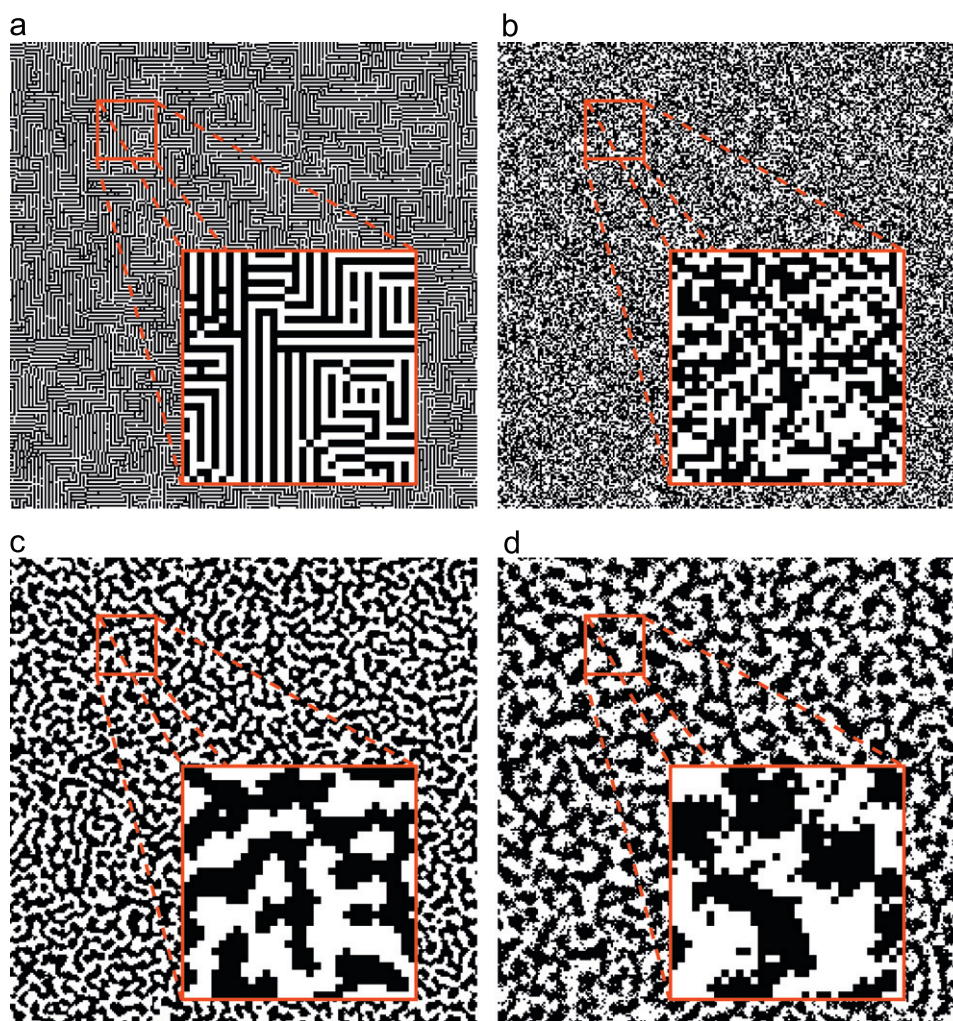


**Fig. 5.** The habitat configurations used for the simulations shown in Figs. 3 and 4. White squares correspond to habitat A, black squares to habitat B. The insets show a  $32 \times 32$  region magnified. All lattices were generated from the same random initial state (which is nearly identical to lattice (b)); only a very small amount of annealing was needed to make  $k$  exactly 0.5) using the annealing method described in Section 3. Lattices (c) and (d) have the same pairwise correlation number  $k=0.75$ , but the different annealing parameters used to generate them lead to visibly different higher order correlations and to corresponding differences in population dynamics. (a)  $k=0.3$ . (b)  $k=0.5$ . (c)  $k=0.75$ ,  $\gamma=10$ . (d)  $k=0.75$ ,  $\gamma=3$ .

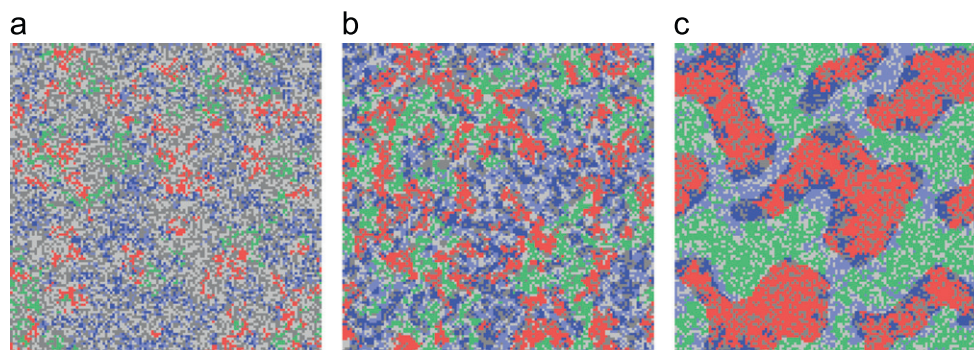


**Fig. 6.** Snapshots of the population equilibrium after a few hundred mean lifetimes for various values of  $k$ , with  $p_g$  near the middle of the coexistence region. Snapshots were taken from simulations run on a  $128 \times 128$  lattice with  $\phi = 4\mu$  and  $\epsilon = 0.001$ . The red and green sites are occupied by a and b specialists, respectively, the blue sites are occupied by generalists and the gray sites are vacant. For the blue and gray colors, darker shades are used for habitat A and lighter shades for habitat B. These snapshots have been taken from interactive Java applets available at <http://vyznev.net/ca/coex2env/>. (a)  $k=0.5$ ,  $p_g=0.43$ . (b)  $k=0.75$ ,  $p_g=0.7$ . (c)  $k=0.95$ ,  $p_g=0.93$ . (For interpretation of the references to color in this figure legend, the reader is referred to the web version of this article.)

equilibrium, with the initial part of the growth curve appearing approximately exponential.

Fig. 7 shows some simulations demonstrating mutual invasibility at six points within the coexistence region of the parameter space. With 100 initial invader individuals, the invader strain

survived and established itself in all runs carried out—evidently the invasion probability of a single invader exceeds  $1/100$  at all the sampled parameter values. The population density of the invading strain over time shows a distinctive sigmoid shape with the initial growth being approximately exponential. A notable

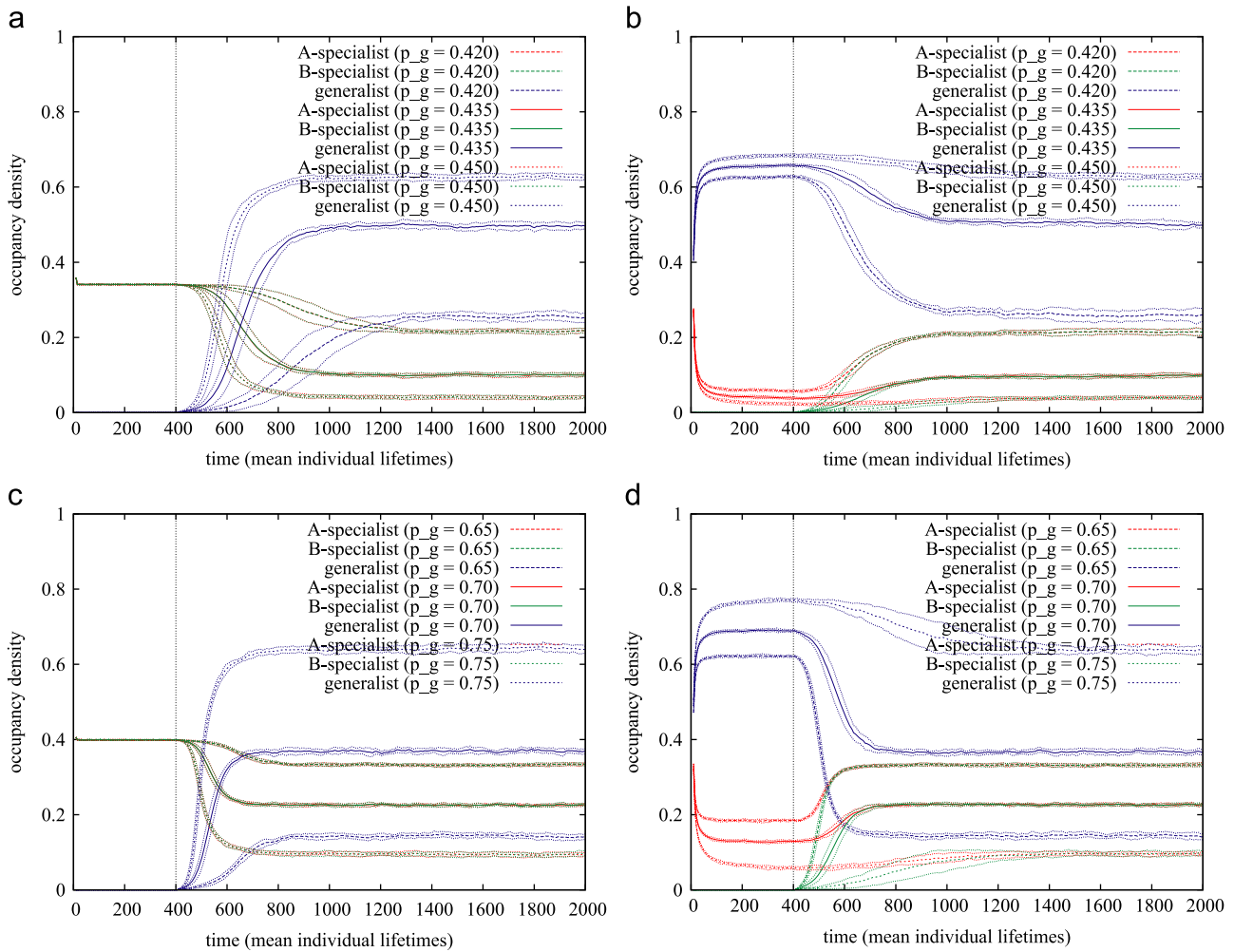


**Fig. 7.** Simulations showing mutual invasibility at the parameter values marked in Fig. 4b and d;  $\phi = 8\mu$  for all simulations. A dimorphic population is allowed to equilibrate for  $400/\mu$  time units, after which 100 individuals (i.e. initial density  $\approx 0.0015$ ) of the third strain are placed randomly on the lattice. In simulations of specialist invasion, the invading strain is without loss of generality taken to be b. The population densities shown in the graphs are smoothed over  $5/\mu$  time units and averaged over 10 independent simulation runs; invasion does succeed in all runs. The red, green and blue lines show the average a, b and g strain densities, respectively, while the solid, dashed and dotted lines correspond to different values of  $p_g$  within the coexistence region. (In populations with both specialist strains present, the red and green lines tend to overlap.) The thin dotted lines are drawn one sample standard deviation above and below the corresponding average line. (a) Generalist invasion ( $k=0.5$ ). (b) Specialist invasion ( $k=0.5$ ). (c) Generalist invasion ( $k=0.75, \gamma=3$ ). (d) Specialist invasion ( $k=0.75, \gamma=3$ ). (For interpretation of the references to color in this figure legend, the reader is referred to the web version of this article.)

feature visible in the plots is that invasion by a specialist strain also increases the population of the other specialist strain already present; this happens because both specialists are in competition with the generalist strain. The relatively high variance seen in some of the plots during the growth phase is due to initial demographic stochasticity affecting the time until exponential growth sets in; once properly started, the shape of the growth curve is very similar in all runs.

Were the coexistence observed in this model merely neutral, the population density of a newly introduced strain would be as likely to decrease as to increase as the result of stochastic fluctuations. The fact that, at the sampled parameter values, small populations of each strain instead show a clear increasing trend confirms that this model exhibits true, non-neutral coexistence.

## 7. Discussion

In this paper I have demonstrated, using a simple toy model of competitive population dynamics on a lattice, that spatial heterogeneity is one of the mechanisms by which the competitive

exclusion principle can be violated. The fact that this cannot occur in well-mixed populations shows that population viscosity and explicit spatial structure are essential to this mechanism.

Had the model included more than two habitat types, temporal variation, hierarchical competition or nonlinear interactions between individuals, the coexistence of multiple strains would not have been at all surprising. Yet it has none of these, and can still support more than two strains in stable coexistence. All that allows such coexistence to persist in this model is the combination of environmental variation, persistent spatial structure and distance-limited dispersal; eliminating any of these reduces the model to one capable of supporting no more strains than would be predicted by a naive application of the competitive exclusion principle.

Real organisms do not usually live in a completely homogeneous environment, nor do most of them disperse uniformly over their entire habitat. It is obvious and commonly acknowledged that environmental variation can increase diversity, yet the fact that, when combined with distance-limited dispersal, this increase can be more than linear seems to have attracted little attention. Yet the ubiquity of habitat edges and fragmented landscapes in nature suggests that it should be possible to find examples of this type of

coexistence in nature, and indeed that such “edge effects” may contribute to the generation and maintenance of ecological diversity in many, if not most, ecosystems.

I find, however, that in many ways this work has raised more questions than it has answered. For example, an obvious question would be whether the model allows the stable coexistence of more than three strains. Another natural question is whether the coexistence of three or more strains in this type of model can also be evolutionarily stable, and further, whether it might arise from a mono- or dimorphic state through evolutionary branching (Geritz et al., 1998; Mágori et al., 2005). Based on limited simulation experiments, the answer to all of these questions appears to be “yes”, although the conditions still need to be explored more thoroughly.

### Acknowledgments

I would like to thank my colleague Robert Service for his comment during a presentation which originally led me to investigate this model, and my advisor Éva Kisdi for her guidance and assistance. I am also grateful to Minus van Baalen for useful discussions and for suggestions regarding the landscape generation algorithm, and to the editor and reviewers of the previous revisions of this paper for their valuable feedback.

This work was financially supported by the Finnish Graduate School in Computational Sciences (FICS).

### References

- Abrams, P.A., 1988. How should resources be counted? *Theor. Popul. Biol.* 33, 226–242.
- Adler, F.R., Mosquera, J., 2000. Is space necessary? Interference competition and limits to biodiversity. *Ecology* 81, 3226–3232.
- Armstrong, R.A., McGehee, R., 1980. Competitive exclusion. *Am. Nat.* 115, 151–170.
- Débarre, F., Lenormand, T., 2011. Distance-limited dispersal promotes coexistence at habitat boundaries: reconsidering the competitive exclusion principle. *Ecol. Lett.* 14, 260–266.
- Dieckmann, U., Metz, J.A.J., 2006. Surprising evolutionary predictions from enhanced ecological realism. *Theor. Popul. Biol.* 69, 263–281.
- Gause, G.F., 1932. Experimental studies on the struggle for existence. *J. Exp. Biol.* 9, 389–402.
- Geritz, S.A.H., Kisdi, E., Meszéna, G., Metz, J.A.J., 1998. Evolutionarily singular strategies and the adaptive growth and branching of the evolutionary tree. *Evol. Ecol.* 12, 35–57.
- Harris, T.E., 1974. Contact interactions on a lattice. *Ann. Probab.* 2, 969–988.
- Hiebeler, D.E., Morin, B.R., 2007. The effect of static and dynamic spatially structured disturbances on a locally dispersing population. *J. Theor. Biol.* 246, 136–144.
- Hsu, S.B., Hubbell, S.P., Waltman, P., 1978. Competing predators. *SIAM J. Appl. Math.* 35, 617–625.
- Jenkins, B., 2007. A small noncryptographic PRNG. <<http://burtleburtle.net/bob/rand/smallprng.html>>.
- Karonen, I. Coupling methods for efficient simulation of contact processes, in preparation.
- Lanchier, N., Neuhauser, C., 2006. A spatially explicit model for competition among specialists and generalists in a heterogeneous environment. *Ann. Appl. Probab.* 16, 1385–1410.
- Levin, D.A., 1970. Competition for pollinators between simultaneously flowering species. *Am. Nat.* 134.
- Mágori, K., Szabó, P., Mizera, F., Meszéna, G., 2005. Adaptive dynamics on a lattice: role of spatiality in competition, co-existence and evolutionary branching. *Evol. Ecol. Res.* 7, 1–21.
- Metz, J.A.J., Mylius, S.D., Dieckmann, O., 2008. When does evolution optimize? *Evol. Ecol. Res.* 10, 629–654.
- Murrell, D.J., Law, R., 2003. Heteromyopia and the spatial coexistence of similar competitors. *Ecol. Lett.* 6, 48–59.
- Neuhauser, C., 1992. Ergodic theorems for the multitype contact process. *Probab. Theory Relat. Fields* 91, 467–506.
- Snyder, R.E., Chesson, P., 2003. Local dispersal can facilitate coexistence in the presence of permanent spatial heterogeneity. *Ecol. Lett.* 6, 301–309.
- Tilman, D., 1982. *Resource Competition and Community Structure*. Monographs in Population Biology. Princeton University Press, Princeton, NJ.
- Tilman, D., 1994. Competition and biodiversity in spatially structured habitats. *Ecology* 75, 2–16.